General comment from the referee:

"The study analyses the influence of cyclones on the tropopause inversion layer. The work builds on previous studies of baroclinic waves and performs of a detailed analysis of cyclone composites using ECMWF analysis data to show the transient behaviour of the static stability maximum. The last part of the study also briefly looks at the possibility that the high vertical shear in the TIL could lead to turbulence. Whilst I think that the study is detailed and interesting, I have several comments that the authors should address before publication."

Authors response:

We thank the reviewer for the careful reading and interest in the study which helped to improve the paper. We reply to every comment in the order as they are listed in the review. We will respond in the following structure: First each comment from the reviewer, followed by our response, and finally the changes in the manuscript. The text coloured in blue are the changes associated with this review, cyan coloured text refers to the second review. The pages and lines indicate the position of the changes in the updated manuscript (the version without color-marked changes).

Comment 1: Cyclone tracking: P5, lines 6 to 11. I appreciated the detailed description of the cyclone tracking algorithm but I am concerned about the effect of the projection and interpolation. The final composited feature in static stability looks like a North-South dipole. I am wondering what the effect of the original grid and interpolation does to this feature. E.g., does it enhance the dipole?

Reply to comment 1: The Lambert projection is solely part of the tracking algorithm. Once the tracks are defined, all data like e.g. the quasi-horizontal fields of the maximum in static stability N^2 above the thermal tropopause are extracted from the original ECMWF latitude-longitude-grid. Therefore the Lambert projection has no effect on the analysis of the North-South dipole feature of the static stability.

The interpolation onto an area-preserving Lambert projection is done based on the work of Hanley and Caballero (2012) who chose this specific projection to counteract the bias in effective zonal resolution when searching for local minima in the mean sea level pressure field (or any field for that reason). The higher zonal resolution at higher latitudes (with reference to the geometric distance between grid points) could be regarded as an advantage, representing denser information, but at the same time it represents an inconsistency between high and low latitudes. The interpolation on to the area preserving Lambert projection with uniform geometric grid (with 28 km grid spacing, representing a form of lowpass-filter for the higher latitudes) counteracts that fact, achieving a more consistent cyclone track density over the whole area.

Comment 2: Composites of cyclones: P6, line 11. Do you mean cylindrical rather than spheric? The data you have is on an equidistant grid (Is this gridding only done for the cyclone tracking or is this gridded data used for the subsequent composites). I am confused about which data is being interpolated to the red pillar since the underlying grey grid in figure 2 is not equidistant.

Reply to comment 2: The basis for the interpolation is defined by the rotation of a spherical polar coordinate surface onto the centre of a tracked cyclone. The pillar of gridded data interpolated on the new rotated grid with the height coordinate dz relative to the tropopause could indeed be described as a cylindrical polar coordinate system. The underlaying grey grid in Figure 2 represents the original latitude-longitude grid as provided by the ECMWF with equidistant latitude and longitude grid spacing, but the geometric distance depends on the latitude (the aforementioned bias in zonal resolution). These original fields are interpolated onto the rotated new spherical coordinates with spherical cap of 15° (red area). This achieves comparable areas independent of where each cyclone centre is located. We reworded the specific paragraph describing the interpolation method as follows:

Changes in the manuscript:

Page 7 Line 4: We select a subset of the gridded data as provided by the ECMWF for each cyclone by rotating the pole

of a spheric polar coordinate system (Θ, ϕ) onto the centre of the cyclone and interpolated the original data onto that new grid. The horizontal resolution of the new coordinate system is set to $0.25°$ and the spherical cap radius to $\Theta_{max} = 15°$ ~~(Fig. 2)~~. The radius is chosen such that all relevant features around the cyclone centre are covered. Figure 2 illustrates the interpolation of the data from the original latitude-longitude grid provided by the ECMWF (light grey area for the whole sphere, dark grey for the limited area used in this study) onto an arbitrarily placed new spherical polar coordinate system (orange area).

Comment 3: LC1 and LC2 case studies: Seeing the case studies is helpful in interpreting the composites. Care should be taken in discussing the static stability strength, particularly with the discontinuities that are seen as a result of the analysis in fig 3c and 5c. I would be interested in seeing the average of N^2 (as opposed to N^2_{max}) in the region 3 km above the tropopause. Side note: Add your definition of N^2_{max} to the caption in Fig 3c.

Reply to comment 3: We agree that a detailed discussion of the sub-synoptic-scale or even sub-meso scale features should be treated with caution when using a certain TIL strength definition, due to the discontinuities described. We nevertheless choose the maximum in N^2 above the tropopause as the TIL-strength definition for this study, because we are working with fine grid spacing data, and we want to highlight the variability of the static stability on different scales on one hand and show the difficulties when working with a certain definition of the TIL-strength on the other hand. The average within a certain vertical extent above the tropopause does not only filter a lot of information by default, but in particular for the feature of N^2 above the tropopause, because we know from previous work that larger maxima in N^2 above the tropopause tend to have a smaller vertical extent. Therefore an average over a defined vertical range above the tropopause could have a particular smoothing effect concerning even the large scale variability. We plotted the average of N^2 within 3 km above the tropopause for our case studies for comparison (Figure R1 and R2). Importantly, the analysis using a 3 km-averaged static stability shows very similar locations of the maximum TIL-structures on a synoptic scale, with the largest values in the regions of cyclonic wrap-up around the cyclone centre of air masses originating from lower latitudes. We did not add these plots to the manuscript, but we added the description of an average-based TIL strength definition at the end of section 2.1, to clarify that we deliberately decided to use another definition. We furthermore added the definition of the TIL strength to the caption in Figure 3.

Changes in the manuscript:

Page 4 Line 18: We ~~do this~~ use this specific TIL strength definition, since the high resolution data shows large variability in the UTLS region, with often several maxima evident above the tropopause. Therefore, we find this definition of the TIL strength to be preferable over e.g. the first maximum in static stability above a threshold (4×10^{-4} s^{-2}, e.g., Gettelman and Wang, 2015). Another way to describe the static stability above the tropopause is to calculate the mean value of N^2 over a predefined vertical extent relative to the tropopause (e.g., Kunkel et al., 2014). While such a TIL strength definition achieves very similar results on a synoptic scale to the ones we will describe in Sect. 3, it also filters a lot of small scale variability and therefore partly neutralises the advantage of analysing high resolution data.

Page 9 Fig. 3 caption: Evolution of a baroclinic wave breaking event as seen in ECMWF IFS analysis data. The middle row represents the 14th of October 2014 at 06:00 UTC~~,~~ (the point in time of maximum cyclone intensity), the upper and lower row show the situation 24 hours prior and past the maximum intensity. Column (a) shows the pressure at mean ~~seal~~ sea level ~~(solid lines $p_{msl} < 1013$ hPa, dashed $p_{msl} > 1013$ hPa, dotted $p_{msl} = 1013$ hPa)~~(solid lines $p_{msl} \leq 1013$ hPa, dashed lines $p_{msl} > 1013$ hPa, in steps of 5 hPa), (b) the IPV on 330 K, (c) the maximum of static static stability N^2_{max} within 3 km above the thermal tropopause as indicator for the TIL strength, and (d) the relative vorticity at lapse rate tropopause height. Blue lines in middle row show 40 and 50 m s^{-1} horizontal windspeed isolines at 200 hPa. Dashed black line shows the path of migration of the tracked cyclone, with the position of the cyclone centre at the point in time of the meteorological field displayed marked by the black x. Black circles show the 15° radius used for the composites. Note the deformation of the circles due to the mercator projection.

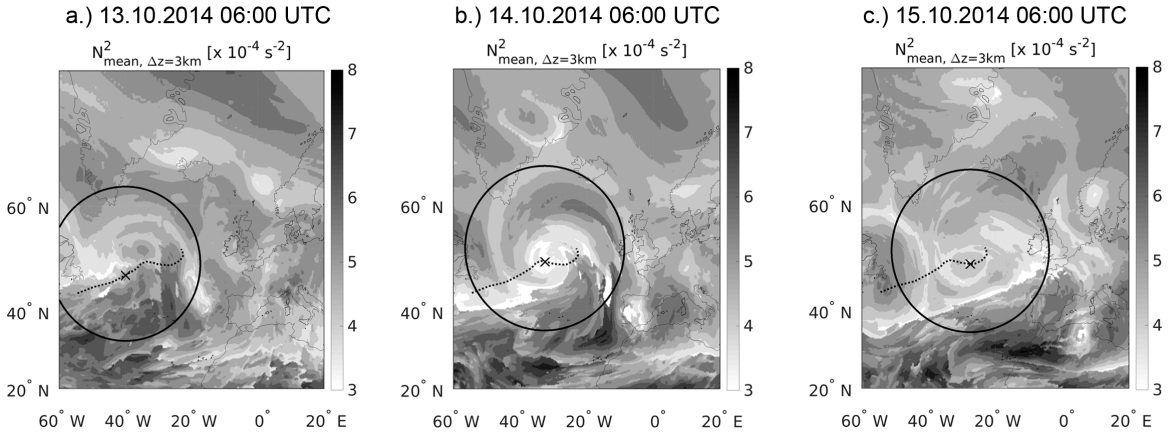

Figure R1. Evolution of the N^2 average based TIL strength for the LC2 resembling baroclinic wave breaking event. The grey contour shows the average of static stability over the vertical extent of 3 km above the thermal tropopause. Figure 1a) shows the TIL strength 24 hours before maximum intensity of the surface cyclone, b) at maximum intensity and c) 24 hours later.

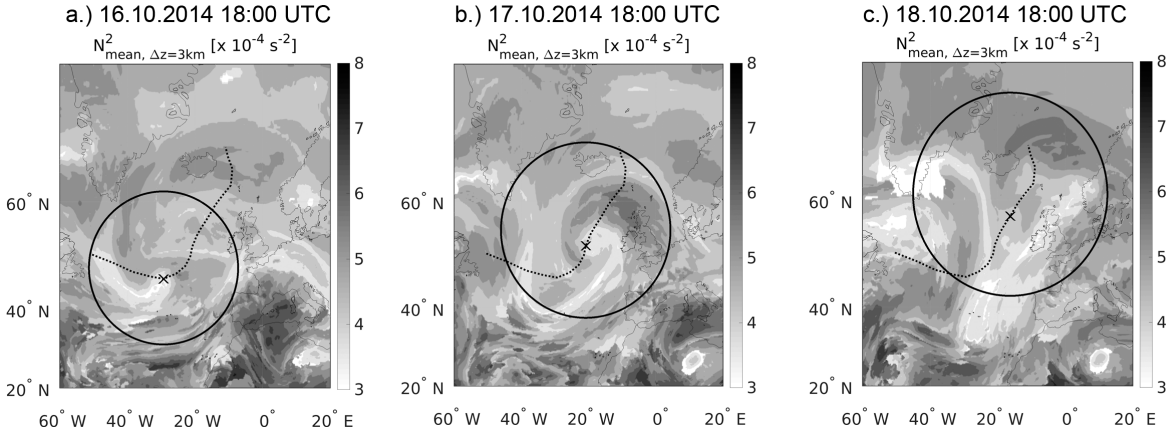

Figure R2. As in Figure R1 but for the LC1 resembling baroclinic wave breaking event.

Comment 4: In figure 4, it may be more helpful to show the cross section at some latitude north of the cyclone centre since this is the region where there is an enhancement in N^2.

Reply to comment 4: We chose this cross-section in particular because it shows the small-scale stratospheric intrusion at around 12° W which is also visible as a discontinuity in the N^2_{max} contour plot in Figure 3 in the middle row. It furthermore covers the tropopause jump between 30° W and 40° W. Both characteristics are the ones described in the paragraph associated with Figure 4. We included an additional cross-section (Figure R3) north of the cyclone centre into the manuscript to furthermore illustrate the variability of N^2 above the tropopause in the region of interest.

Changes in the manuscript:
Page 10 Line 25: The vertical cross-section in Fig. 4b shows the TIL structures at 60° N on the same day and north of the cyclone centre. It illustrates that the regions of enhanced static stability exhibit less variability at this latitude. They are located above the ridge between 40° W and 10° W, with the wave-like horizontal pattern that is also visible in Fig. 3c.

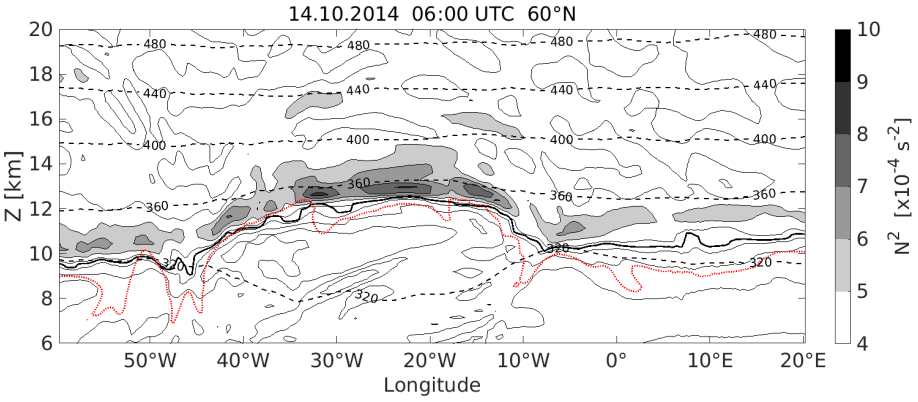

Figure R3. Vertical crosssection over the North Atlantic on 14.10.2014 at 06:00 UTC at 60° N. The filled contour as well as the thin solid black contour lines show static stability N^2 in steps of $1 \times 10^{-4}\mathrm{s}^{-2}$, dashed black lines show isentropes. The bold solid black line indicates the lapse rate tropopause, the dotted red line shows the 2 pvu isoline of potential vorticity.

Comment 5: Composite analysis: I have some concerns about the compositing the values of N^2_{max} and artefacts that might arise as a result of this. Have you looked at a number of cyclones in your composite to make sure that the features in N?2 are indeed present in most of them?

Reply to comment 5: This is a very valid concern which we shared during the data evaluation, especially since we know about the sensitivity of the result on the TIL-strength definition. We did in fact look at a large number of cyclones independently. While there is a large variability in the evolution of the upper tropospheric / lower stratospheric wrap-up around the cyclone centre (caused by the variability of the background flow, the cyclone evolution and the wave activity in the UTLS, as well as the variety of mechanism which influence the static stability at tropopause altitude). Most of the cyclones and especially the strong ones exhibit a comparable evolution of the static stability above the tropopause, with the wrapped-up North-South-dipole as the synoptic to mesoscale shaping. We furthermore estimate the mentioned discontinuities in the TIL-strength due the reasons described in the last paragraph of subsection 3.1 to be small and infrequent enough to be negligible for the large scale composite analysis. We updated Figure 11 and added Fig 12 to the manuscript with a set of vertical tropopause-based

cross-section composites of S^2 and N^2, which further illustrate the issue in a more comprehensive way. The plots complement Figure 9 and Figure 10b for different rotation angles around the cyclone centre, and while all these cross-section composites are solely based on the lapse rate tropopause definition, they do agree very well with the composites derived from the quasi-horizontal fields of the individual cyclones that depend on the definition of the TIL-strength and the strength of the wind shear (maximum of N^2 (Fig. 7b) / S^2 (Fig. 12) within 3 km above the tropopause). We added a description of this comparison to the manuscript.

Changes in the manuscript:

Page 19 Figure 11 caption: ~~Composite of flow features for the 76 strong cyclones with $p_{msl,\,min} \leq 990$ hPa at the point in time of maximum intensity. Left panel: composite of the maximum in vertical wind shear S^2_{max} found within 3 km above the lapse rate tropopause for each cyclone. The black arrow indicates the position of the vertical cross-sections in Fig. 9. Right panel: composite of the absolute height difference between the maximum in static stability N^2_{max} and the maximum in vertical wind shear S^2_{max}, both within 3 km above the lapse rate tropopause.~~ Composite of the vertical wind shear for the 76 strong cyclones with $p_{msl,\,min} \leq 990$ hPa at the point in time of maximum intensity, averaged over the individual quasi-horizontal fields of maximum vertical wind shear S^2_{max} found within 3 km above the lapse rate tropopause for each cyclone. The black arrows indicate the orientation of the vertical cross-sections in Fig. 12.

Page 20 Figure 12 caption: Composites of flow features for the 76 strong cyclones with $p_{msl,\,min} \leq 990$ hPa at the point in time of maximum intensity. Vertical tropopause-based averaged cross-section composites, reaching from the cyclone centre (a) northwestward, (b) southwestward, (c) southeastward and (e) northeastward. Top row shows static stability N^2 and cloud ice water content as in Fig. 9, bottom row shows wind shear S^2 as in Fig. 10b. The orientation of the vertical cross-sections is indicated by the black arrows in Fig. 11.

Page 18 Line 9: ~~Figure 12 provides a strong indication that a co-location between the regions of enhanced static stability above the tropopause and the maximum in vertical shear of the horizontal wind exists. Figure 12a shows the quasi-horizontal composite of the maximum in wind shear within 3 km above the tropopause for the subset of strong cyclones ($p_{msl,\,min} \leq 990$ hPa). It reveals together with Fig. 7 that there is a co-location between the regions of maximum squared wind shear S^2_{max} above the tropopause and the regions of maximum enhancement in static stability N^2_{max} in the lower stratosphere. Figure 12 furthermore shows how both features are also vertically constrained north of the cyclone centre, resulting in the vertical overlap of the wind shear region and the TIL (see also Fig. 9 and Fig. 10b).~~

Figure 11 further illustrates the connection between the regions of enhanced static stability and the vertical shear of the horizontal wind in the vicinity of cyclones. It shows the composite derived from the quasi-horizontal fields of maximum wind shear S^2_{max} found within 3 km above the tropopause in the 76 strong cyclones. The region of largest mean wind shear matches with the region of maximum enhanced static stability (see Fig. 7b), with maximum values north and northeast of the cyclone centre within the wrapped-up ridge. The southern regions exhibit weaker mean wind shear, and the minimum values of S^2_{max} are located around the cyclone centre.

Figure 12 shows tropopause based averaged vertical cross-sections that cover the distance from the cyclone centre to the spherical cap radius of 15° and are oriented in different cardinal directions as indicated in Fig 11. These plots complement Fig. 10b and Fig. 11 and further confirm a co-location as well as a co-occurence of the regions of maximum wind shear S^2_{max} and the regions of maximum enhanced static stability N^2_{max}. They furthermore illustrate the validity and representativity of the composites derived from the individual quasi-horizontal fields. The quasi-horizontal composite in Fig. 7b strongly depends on the definition of the TIL-strength (in this case the maximum value of N^2 within 3 km above the tropopause), while the vertical cross-section composites in the top row of Fig. 12 solely depend on the tropopause definition (equivalently Fig. 11 and Fig. 12 bottom row for the vertical wind shear). However, both methods show a good agreement, aside from an overall shift of the absolute values as expected and described in Sect. 2.2.1.

Comment 6: Richardson number analysis: I find this very interesting. Do the corresponding plots for the case studies in section 3 show very low values of Ri above the tropopause (regions with $Ri < 1$)?

Reply to comment 6: The regions of enhanced static stability within the individual cyclones are mostly dominated by large vertical shear of the horizontal wind which results in low Richardson numbers despite the enhanced N^2, as is the case for the LC1 and LC2 case study (Figure R4). Several cyclones in our dataset exhibit regions with even very low Richardson numbers ($Ri < 1$) at tropopause altitudes, in anticyclonic upper tropospheric flow inside the ridge of the baroclinic waves and with partial overlap into the regions of enhanced static stability. These regions however appear as transient and localised features. A detailed analysis of such a case is subject to a corresponding study we are working on, which is in preparation to be submitted to ACPD.

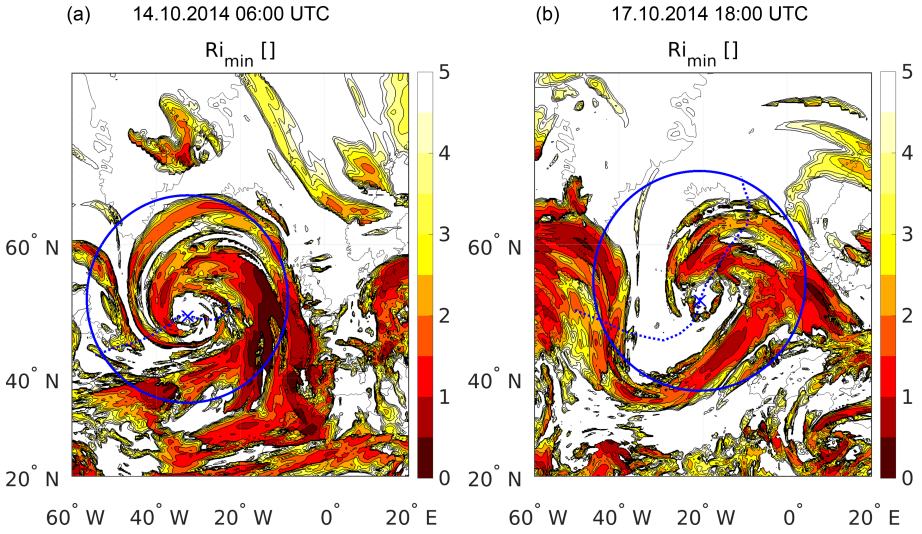

Figure R4. Minimum Richardson numbers Ri_{min} within 3 km above the thermal tropopause, at the point in time of maximum cyclone intensity a.) for the LC2 resembling baroclinic wave, and b.) for the LC1 resembling baroclinic wave.

Comment 7: P18 line 31. The Richardson numbers found are not low enough for turbulent flow. I would suggest not making such a strong statement in the conclusion.

Reply to comment 7: We rephrased the paragraph to make the statement less strong and to clarify that we do not expect the whole region to be dynamically unstable (because the Richardson numbers are still too large as you pointed out). We rather want to note that the general tendency towards high vertical wind shear in the region of interest (considering the variability of N^2 and S^2) points toward the possibility for localised turbulence.

Changes in the manuscript:

Page 21 Line 11: Mean Richardson numbers calculated for these flow conditions ~~favourable for turbulence~~ reveal a region of local minima in Ri right above the tropopause at around 5° north from the cyclone centre in the composite. ~~This result points toward a co-location between an enhancement in static stability above the tropopause and potential turbulent mixing of tropospheric and stratospheric air masses (Kunkel et al., 2016).~~ Taking into account the variability of N^2 and S^2 for individual cyclones, this result points toward the possibility of a co-location between enhanced static stability above the tropopause and

localised regions of turbulent mixing of tropospheric and stratospheric air masses (Kunkel et al., 2016).

Comment 8: The colour scale on some of the figures could be chosen to be slightly more intuitive. E.g., Fig 10 (c) At first glance, I thought the red values were bigger.

Reply to comment 8: We agree that this plot can be counterintuitive due to the inverted color scale, but we want to highlight the region with the tendency toward turbulent motion (i.e. low Richardson numbers) and therefore want to keep the inverted colors for this particular Figure. We added a note on this to the Figure caption. We furthermore changed the color scale to a lower maximum value to make the plot more easy to read.

Changes in the manuscript:

Page 18 Fig. 10 caption: Vertical tropopause-based averaged cross-section as in ~~Figure 8~~Fig. 9, but only north of the cyclone centre. Left panel: filled contours show mean vertical velocity, solid thin black line the $\omega = 0$ Pa s^{-1} isoline. Grey dashed lines are isolines of the cloud ice water content, steps as in Fig. 9. Middle panel: filled contour and solid black contour lines show squared vertical shear of horizontal wind S^2. Right panel: modified Richardson number mean Ri, with an inverted color scale (red represents low values) to highlight the tendency toward turbulent motion. ~~Grey~~Blue solid bold line in all three panels shows the $N^2_{mean} = 6 \times 10^{-4}$ s^{-2} isoline, dashed black lines the isentropes.

Other comments: P2, line 31. Fix reference - P4 line 3 "the a more", line 25 "oder" - P6 line 6, "North Africa an the" - P9 caption a) "seal level" - P12 line 7 "extend" - P13 lines 17 and 18 "This region of strong with..." Meaning unclear. - P14 line 8 "stronger" to more pronounced - P 16 fig 10 caption "Vertical crosssection as in figure 8" should be figure 9. also "north the cyclone", "of" missing.

Reply: We fixed the mistakes in the manuscript.

References

Gettelman, A. and Wang, T.: Structural diagnostics of the tropopause inversion layer and its evolution, Journal of Geophysical Research Atmospheres, 120, 46–62, https://doi.org/10.1002/2014JD021846, 2015.

Hanley, J. and Caballero, R.: Objective identification and tracking of multicentre cyclones in the ERA-Interim reanalysis dataset, Quarterly Journal of the Royal Meteorological Society, 138, 612–625, https://doi.org/10.1002/qj.948, 2012.

Kunkel, D., Hoor, P., and Wirth, V.: Can inertia-gravity waves persistently alter the tropopause inversion layer?, Geophysical Research Letters, 41, 7822–7829, https://doi.org/10.1002/2014GL061970, 2014.

WMO: Meteorology - A three dimensional science, WMO Bulletin, pp. 134–138, 1957.